



Murine Intrarectal Instillation of Purified Recombinant *Clostridioides difficile* Toxins Enables Mechanistic Studies of Pathogenesis

 Nicholas O. Markham,^{a,b} Sarah C. Bloch,^c John A. Shupe,^c Erin N. Laubacher,^{a,b} Audrey K. Thomas,^c Heather K. Kroh,^c Kevin O. Childress,^c F. Christopher Peritore-Galve,^c M. Kay Washington,^c Robert J. Coffey,^{a,b}  D. Borden Lacy^{b,c,d}

^aDivision of Gastroenterology, Vanderbilt University Medical Center, Nashville, Tennessee, USA

^bEpithelial Biology Center, Vanderbilt University School of Medicine, Nashville, Tennessee, USA

^cDepartment of Pathology, Microbiology, and Immunology, Vanderbilt University Medical Center, Nashville, Tennessee, USA

^dDepartment of Veterans Affairs Medical Center, Nashville, Tennessee, USA

Nicholas O. Markham, Sarah C. Bloch, and John A. Shupe contributed equally to this study. N.O.M. prepared drafts of manuscript and figures, S.C.B. performed over 100 intrarectal instillations and dissections, and J.A.S. performed and coordinated animal experiments and tissue analysis.

ABSTRACT *Clostridioides difficile* is linked to nearly 225,000 antibiotic-associated diarrheal infections and almost 13,000 deaths per year in the United States. Pathogenic strains of *C. difficile* produce toxin A (TcdA) and toxin B (TcdB), which can directly kill cells and induce an inflammatory response in the colonic mucosa. Hirota et al. (S. A. Hirota et al., *Infect Immun* 80:4474–4484, 2012) first introduced the intrarectal instillation model of intoxication using TcdA and TcdB purified from VPI 10463 (VPI 10463 reference strain [ATCC 43255]) and 630 *C. difficile* strains. Here, we expand this technique by instilling purified, recombinant TcdA and TcdB, which allows for the interrogation of how specifically mutated toxins affect tissue. Mouse colons were processed and stained with hematoxylin and eosin for blinded evaluation and scoring by a board-certified gastrointestinal pathologist. The amount of TcdA or TcdB needed to produce damage was lower than previously reported *in vivo* and *ex vivo*. Furthermore, TcdB mutants lacking either endosomal pore formation or glucosyltransferase activity resemble sham negative controls. Immunofluorescent staining revealed how TcdB initially damages colonic tissue by altering the epithelial architecture closest to the lumen. Tissue sections were also immunostained for markers of acute inflammatory infiltration. These staining patterns were compared to slides from a human *C. difficile* infection (CDI). The intrarectal instillation mouse model with purified recombinant TcdA and/or TcdB provides the flexibility needed to better understand structure/function relationships across different stages of CDI pathogenesis.

KEYWORDS *Clostridioides difficile*, acute colitis, bacterial toxin, mouse model

Clostridioides difficile infection (CDI) is a potentially life-threatening cause of antibiotic-associated diarrhea and is the most common nosocomial disease in the United States (1, 2). The incidence of recurrent CDI, or repeat infection in the same patient, is increasing at an alarming rate and has contributed to the Centers for Disease Control and Prevention (CDC)'s designation of CDI as an urgent threat (3, 4). Widespread infection control and antibiotic stewardship programs have helped reduce the burden of hospital-acquired CDI, but community-acquired infections are becoming more common (5, 6). A better fundamental understanding of CDI pathogenesis is needed to formulate new preventive and therapeutic strategies (7).

C. difficile is a Gram-positive, spore-forming bacterium with obligate anaerobic metabolism (8). CDI is a toxin-mediated disease primarily driven by *C. difficile* toxin A

Citation Markham NO, Bloch SC, Shupe JA, Laubacher EN, Thomas AK, Kroh HK, Childress KO, Peritore-Galve FC, Washington MK, Coffey RJ, Lacy DB. 2021. Murine intrarectal instillation of purified recombinant *Clostridioides difficile* toxins enables mechanistic studies of pathogenesis. *Infect Immun* 89:e00543-20. <https://doi.org/10.1128/IAI.00543-20>.

Editor Victor J. Torres, New York University School of Medicine

Copyright © 2021 American Society for Microbiology. All Rights Reserved.

Address correspondence to D. Borden Lacy, borden.lacy@vumc.org.

Received 29 August 2020

Returned for modification 18 September 2020

Accepted 9 January 2021

Accepted manuscript posted online 19 January 2021

Published 17 March 2021

(TcdA) and toxin B (TcdB) with less potent contribution by the binary transferase toxin (CDT) (9–11). TcdA and TcdB have intracellular glucosyltransferase activity targeting RhoA, Rac1, and CDC42 (12, 13). This inhibitory modification of Rho family GTPases leads to actin depolymerization and disruption of cell-cell junctions (14, 15). Although TcdA and TcdB share 49% amino acid sequence identity and 69% similarity, they have different potencies and mechanisms in multiple animal models (16). When directly compared in porcine explants, both TcdA and TcdB caused glucosyltransferase-dependent apoptosis, but only TcdB could induce a glucosyltransferase-independent cell necrosis at higher concentrations (17–19).

Here, we describe how purified recombinant TcdA and TcdB affect mouse colon after intrarectal instillation. Importantly, our optimized methodology reveals acute inflammatory colitis with low concentrations of either TcdA or TcdB. Whereas these low concentrations induce mild colitis, more aggressive pathology mimicking severe human CDI is observed at higher concentrations of TcdB. The instillation of TcdB mutant toxins reveals the critical roles of endosomal pore formation and glycosylation for initiating *in vivo* mucosal injury in the mouse. Immunofluorescent images reveal how wild-type TcdB disrupts the luminal surface epithelium. Combinations of low-quantity TcdA and TcdB induce acute inflammatory infiltration that is detected using Ly6G (lymphocyte antigen 6G [murine myeloid cell marker]) immunohistochemistry (IHC) more accurately than by hematoxylin and eosin (H&E) staining.

RESULTS

Purified recombinant TcdB reproduced human pathology. To test whether intrarectal instillation of purified recombinant *C. difficile* toxin results in pathology similar to infection with *C. difficile* bacteria, we compared colonic mucosa from this mouse model to the spore gavage infection mouse model and human CDI. Separate blocks of archived formalin-fixed, paraffin-embedded tissue were obtained from four patients with CDI-induced pseudomembranous colitis. At 4 h after instillation of 50 μ g of TcdB, the distal mouse colon was removed and prepared for H&E staining, which showed focal acute inflammation, edema, and apoptosis similar to the severity seen in human CDI (Fig. 1A, left column). Pseudomembrane formation, a hallmark of CDI pathology, was seen even at this early time point in the TcdB instillation model but not the R20291 infection (spore-gavage) model (black arrowheads, Fig. 1A). The 4-h instillation was chosen to evaluate the initial impact of toxin-mediated epithelial damage. The mice develop severe tissue pathology at this time point without observable morbidity or mortality.

To highlight the neutrophil infiltration for comparison to human CDI, sections of tissue were stained with IHC using anti-myeloperoxidase (MPO) antibodies (Fig. 1A, right column). In focal areas of TcdB-instilled mouse colon tissue, MPO⁺ cells infiltrated the lamina propria and epithelium similarly to the human CDI tissue (Fig. 1A, right column). Across the whole distal colon, there appeared to be fewer total MPO⁺ cells per crypt, which may reflect the larger range and patchy distribution of immune infiltration in human colitis (Fig. 1B). The histopathological damage and immune infiltration seen here support intrarectal instillation of 50 μ g of TcdB as a model for human CDI.

TcdB induced colitis and was concentration dependent. We chose to focus primarily on TcdB because preclinical models of CDI with isogenic knockout strains have shown how TcdB is required for inducing wild-type levels of tissue damage and mortality (10, 11, 20). Furthermore, clinical epidemiological data have revealed a worldwide emergence of *C. difficile* strains with only TcdB and not TcdA or transferase toxin (21–24). Hirota et al. first developed the *C. difficile* intrarectal intoxication model using toxins purified from laboratory culture supernatants through dialysis tubing (25). Using recombinant, chromatography-purified TcdB, we performed intrarectal instillations in C57BL/6J mice with a total volume of 200 μ l. Notably, we instilled a higher total volume than the original model (100 μ l) because the potential pipetting error or anal leakage of 10% would result in a lower absolute amount of toxin lost. A blinded, board-certified gastrointestinal pathologist scored the edema, inflammation, and epithelial injury

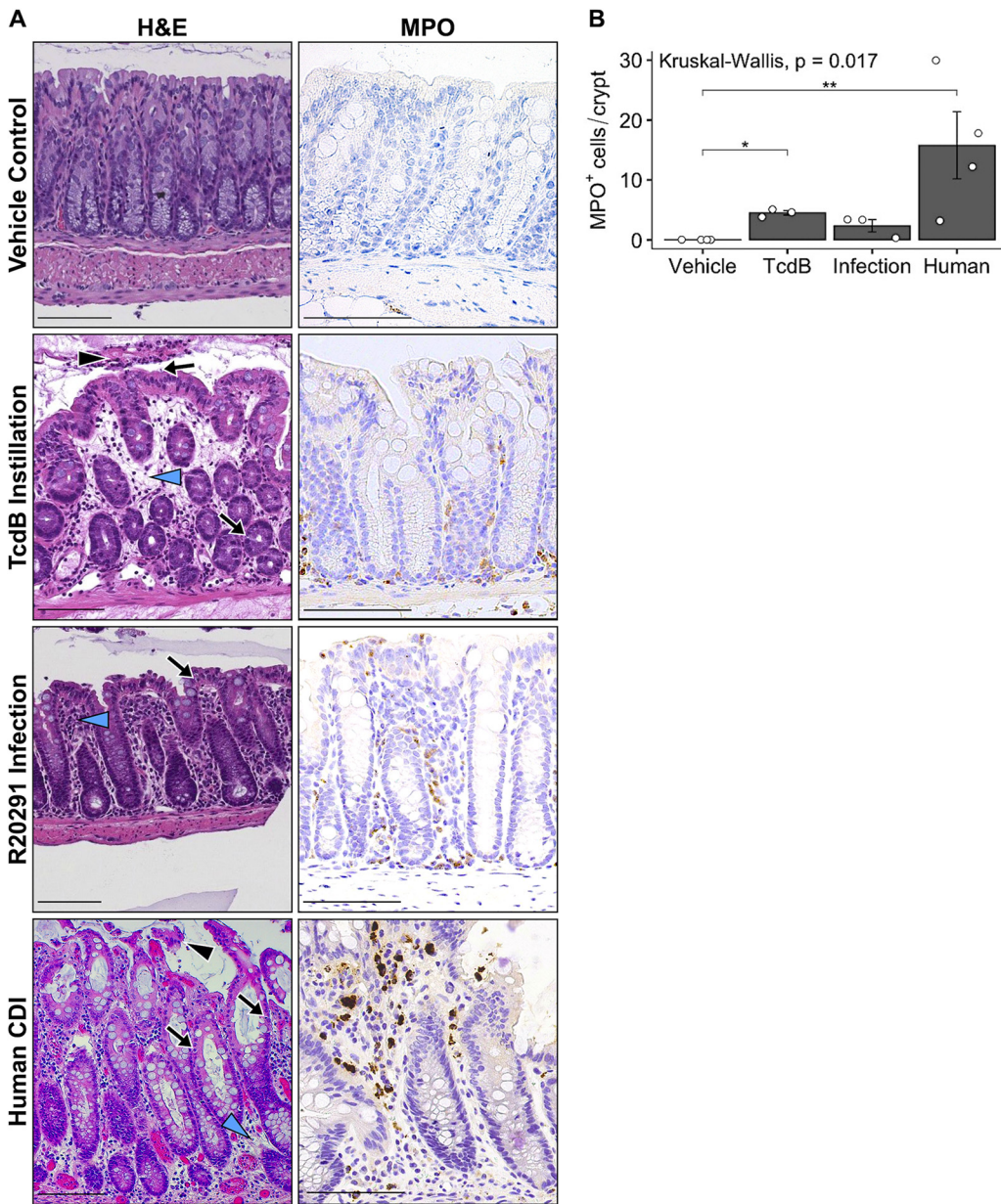


FIG 1 Intrarectal instillation of purified recombinant TcdB recapitulates the histopathology of human CDI. (A) Images from H&E staining and MPO IHC of distal colon epithelium. Distal mouse colon 4 h after instillation of recombinant TcdB (50 μ g/200 μ l) exhibits acute inflammatory infiltration and edema (blue arrowhead), epithelial cell apoptosis (arrows), and pseudomembrane formation (black arrowhead). Infection with R20291 *C. difficile* spore gavage exhibited similar histopathology 4 days postinoculation with notably less edema. Human colonic epithelium from a patient with CDI and pseudomembranous colitis shows severe acute inflammatory infiltration and edema (blue arrowhead), epithelial cell apoptosis (arrows), and pseudomembrane formation (black arrowhead). Scale bars, 100 μ m. (B) Quantification of MPO⁺ cells per crypt, $\eta^2 = 0.714$ (large effect size for Kruskal-Wallis test), $n = 4$ mice/group. Error bars show standard errors of the mean (SEM), and each open circle represents the average MPO⁺ cells per crypt from 10 fields of view at $\times 20$ magnification for a single mouse. Significantly different groups as determined by Dunn's test are shown in brackets (*, $P \leq 0.05$; **, $P \leq 0.01$).

according to published criteria (26). In contrast to Hirota et al., we saw significant edema and inflammation with 5 μ g of TcdB (Fig. 2). This quantity also appeared to induce epithelial injury, but this histopathological subscore did not reach statistical significance compared to vehicle control ($P = 0.07$). Even 0.5 μ g of TcdB instillation appeared to induce edema and inflammation, but again the histopathological scores were not significantly different from control ($P = 0.14$ and $P = 0.08$, respectively). Increasing the quantity of TcdB

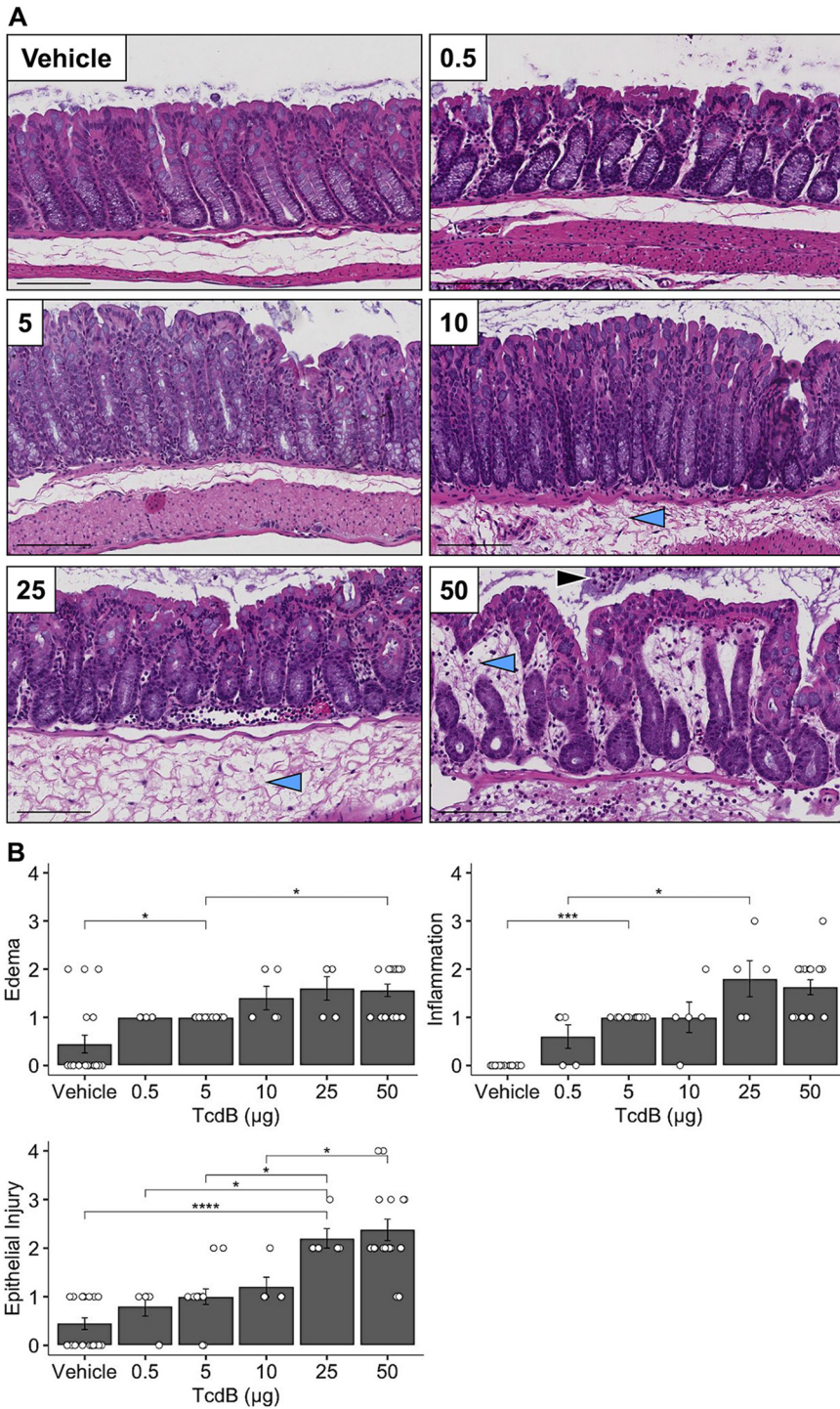


FIG 2 Purified recombinant TcdB induces colitis at low doses and is dose dependent. (A) At 4 h after intrarectal instillation of TcdB (total µg/200 µl shown as an inset), mouse colons were prepared for H&E as in Fig. 1. Vehicle negative control was either PBS or HBSS. Representative images are shown from each group. Pseudomembrane formation (black arrowhead), edema (blue arrowheads). Scale bar, 100 µm. (B) Histopathological scoring by an expert gastrointestinal pathologist blinded to the conditions was recorded as mean score per group. Error bars indicate the SEM ($n=5$ to 18 mice/group, each open circle is one animal). All three subscores were significant as determined by the Kruskal-Wallis test with large effect size: edema, $P = 9.4 \times 10^{-5}$ and $\eta^2 = 0.373$; inflammation, $P = 5.7 \times 10^{-9}$ and $\eta^2 = 0.75$; and epithelial injury, $P = 9.4 \times 10^{-8}$ and $\eta^2 = 0.643$. Post hoc analysis with Dunn's test generated P values (*, $P \leq 0.05$; **, $P \leq 0.01$; ***, $P \leq 0.001$), as indicated. Not all significant comparisons are shown in order to avoid overplotting.

induced increased damage in all three subscores, with 25 and 50 μg of TcdB having had the largest effect (Fig. 2). These two treatments resulted in similar histopathological scores, but only mice in the 50- μg TcdB group developed early pseudomembrane formation (12.5%, $n=2/16$) composed of sloughed epithelial cells, neutrophils, and fibrin debris in the lumen (Fig. 2A, black arrowhead). With regard to the edema score, it was frequently difficult to differentiate mild edema from tissue sectioning artifact when space was seen between the lamina propria and muscularis mucosa. None of the mice had physiological changes, such as hunched posture or diarrhea, at the 4-h time point used in this study. The edema and inflammation observed with 5 μg of TcdB and its dose-dependent effect highlight the robustness of this model for studying mild to severe disease.

Mutant TcdB instillation revealed structure/function relationship. To determine the functional impact of specific TcdB components, we performed intrarectal instillation with 50 μg of either wild-type, L1106K (a mutant lacking pore-forming function), or D286/288N (referred to here as DxD [D286/288N mutant lacking glucosyltransferase]) TcdB. The L1106K mutation ablates a hydrophobic region in the TcdB translocation domain, thus prohibiting pore formation in intracellular endosomes and the subsequent release of the glucosyltransferase domain into the cytosol (27, 28). The DxD motif mutation blocks the TcdB glucosyltransferase catalytic site from binding UDP-glucose and manganese cosubstrates, therefore inhibiting the enzymatic activity of the glucosyltransferase domain (17, 29–31). Histopathological scoring of H&E-stained tissue showed L1106K and DxD mutant TcdB toxins giving similar damage scores compared to vehicle control (Fig. 3A). Although not statistically different than vehicle control ($P = 0.43$), the DxD mutant did appear to induce mild acute inflammation (Fig. 3A and B). In the course of these experiments, we directly compared phosphate-buffered saline (PBS) and Hanks' buffered salt solution (HBSS) as diluents for the purified toxins. Unpublished work from our lab suggested there might be a buffer-dependent difference in TcdB potency *in vitro*; however, with 5 μg of TcdB, either diluent resulted in the same effect (Fig. 3C). Similarly, cefoperazone pretreatment, which is commonly used in the *C. difficile* spore gavage mouse model, did not cause any significant difference in histopathology compared to water-only controls (Fig. 3D).

Histopathological damage occurred near the lumen without crypt base changes. In a CDI mouse model using oral gavage of infectious spores, adherens junction instability was described throughout the crypt axis from base to lumen (32). We used immunofluorescent staining to examine adherens junctions and the apical brush border after intrarectal intoxication. In Fig. 4A, E-cadherin and Villin immunofluorescence were used to highlight TcdB-induced alterations at the colonic epithelial luminal border. Specifically, the luminal invaginations appeared more numerous and larger in size, and the staining intensity within individual cell membranes appeared to vary. Qualitative changes in the amount of membrane protein sodium-potassium ATPase ($\text{Na}^+/\text{K}^+-\text{ATP}$) and sodium-potassium-chloride channel (NKCC) were also observed (Fig. 4B). However, the mean pixel intensity throughout the distal colonic epithelium was unchanged across mouse groups (Fig. 4C). In addition to comparing TcdB from the VPI 10463 reference strain, we also performed instillations with the L1106K mutant. As we showed in Fig. 3, the L1106K mutant has the same histopathological and epithelial cell membrane effect as the vehicle negative control (Fig. 4C). These data illustrate how the more lumenally located epithelial cells are first affected in the colonic epithelium.

TcdA and TcdB combination induced subtle acute inflammation. To continue leveraging our ability to see tissue damage with low quantities of toxin, we sought to describe the effect of combining TcdA and TcdB in this model. Recombinant wild-type TcdA from the VPI 10463 reference strain gene was prepared and purified similarly to TcdB. Both were instilled either separately or together for 4 h, and tissues were processed by H&E staining and IHC for the Ly6G mouse antigen to identify myeloid-derived cells (33) (Fig. 5A). The IHC staining shows more Ly6G⁺ cell infiltration after TcdB alone than with an equivalent quantity of only TcdA (Fig. 5A and C). Moreover, 5 μg of TcdB added to either 1 or 5 μg of TcdA increased the number of Ly6G⁺ cells per crypt (Fig. 5C). These findings suggest TcdB has a greater impact than TcdA on recruitment of

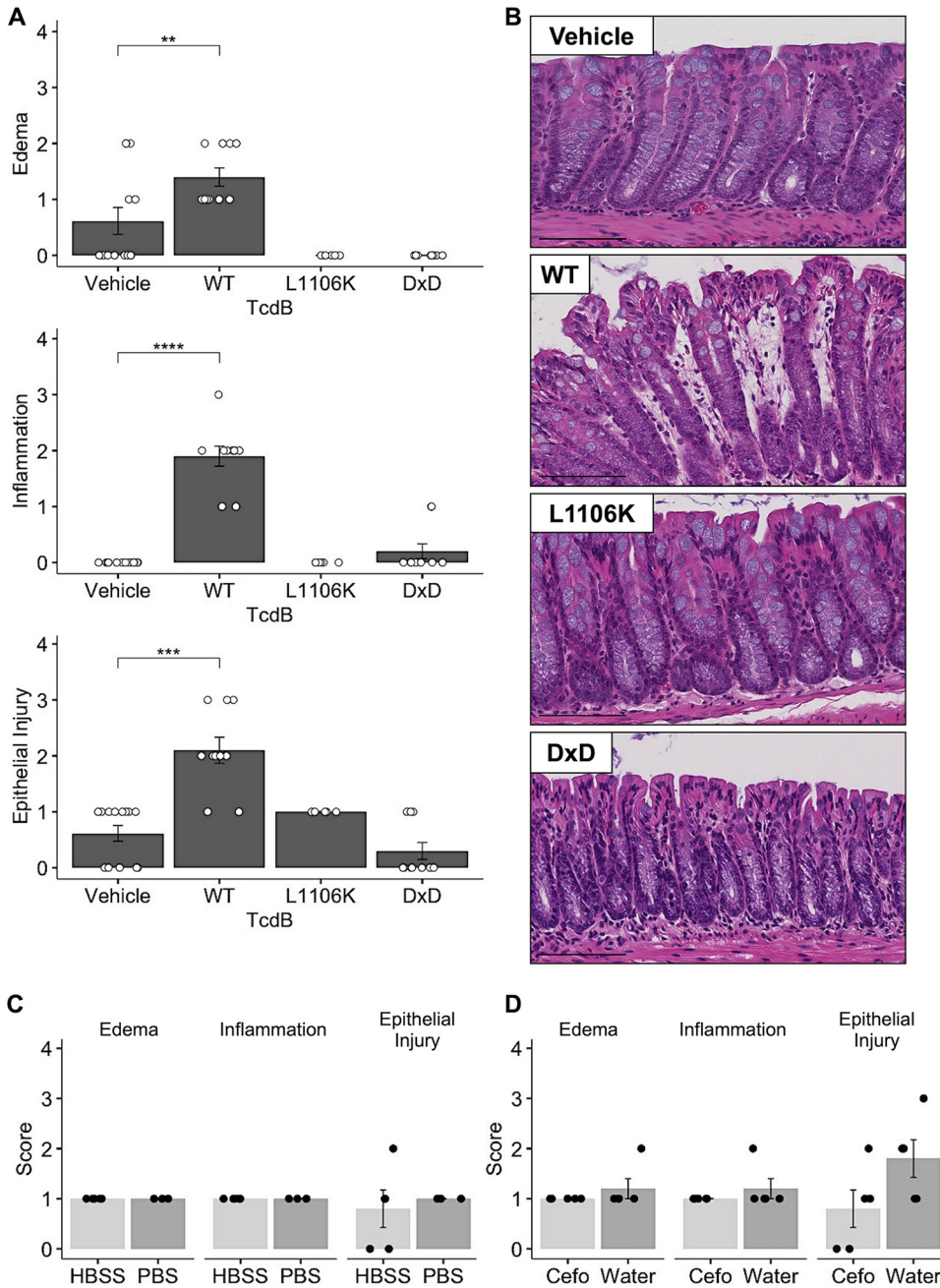


FIG 3 Mutant TcdB toxins lacking pore formation or glucosyltransferase activity fail to induce damage. Recombinant wild-type TcdB from the VPI 10463 reference strain (WT) was produced in *B. megaterium* in parallel with mutant versions L1106K and DxD, which lack endosomal pore formation and glucosyltransferase activity, respectively. (A) Histopathological scores for each group. Error bars indicate the SEM ($n=5$ to 13 mice/group instilled with $50\mu\text{g}$ of toxin). Each open circle represents one animal. All three subscores achieved significance by the Kruskal-Wallis test with a large effect size: edema, $P = 7.2 \times 10^{-5}$ and $\eta^2 = 0.553$; inflammation, $P = 5.8 \times 10^{-7}$ and $\eta^2 = 0.847$; and epithelial injury, $P = 3.7 \times 10^{-5}$ and $\eta^2 = 0.594$. *Post hoc* analysis with Dunn's test generated P values (**, $P \leq 0.01$; ***, $P \leq 0.001$; ****, $P \leq 0.0001$), as indicated. Not all significant comparisons are shown with brackets to avoid overplotting. (B) Representative H&E images from each group. Scale bars, $100\mu\text{m}$. (C) Histopathological scores of mouse colonic tissue 4 h after TcdB ($5\mu\text{g}$) was intrarectally instilled using either HBSS or PBS as diluent ($n=3$ to 5 mice/group; error bars indicate the SEM). Mann-Whitney testing showed no significant differences between conditions. (D) Histopathological scores comparing mice pretreated with either cefoperazone (0.5 mg/ml) or water control for 5 days prior to intrarectal instillation with TcdB ($5\mu\text{g}$) in HBSS for 4 h ($n=5$ mice/group, each black circle is one mouse; error bars indicate the SEM). Mann-Whitney testing showed no significant differences between conditions.

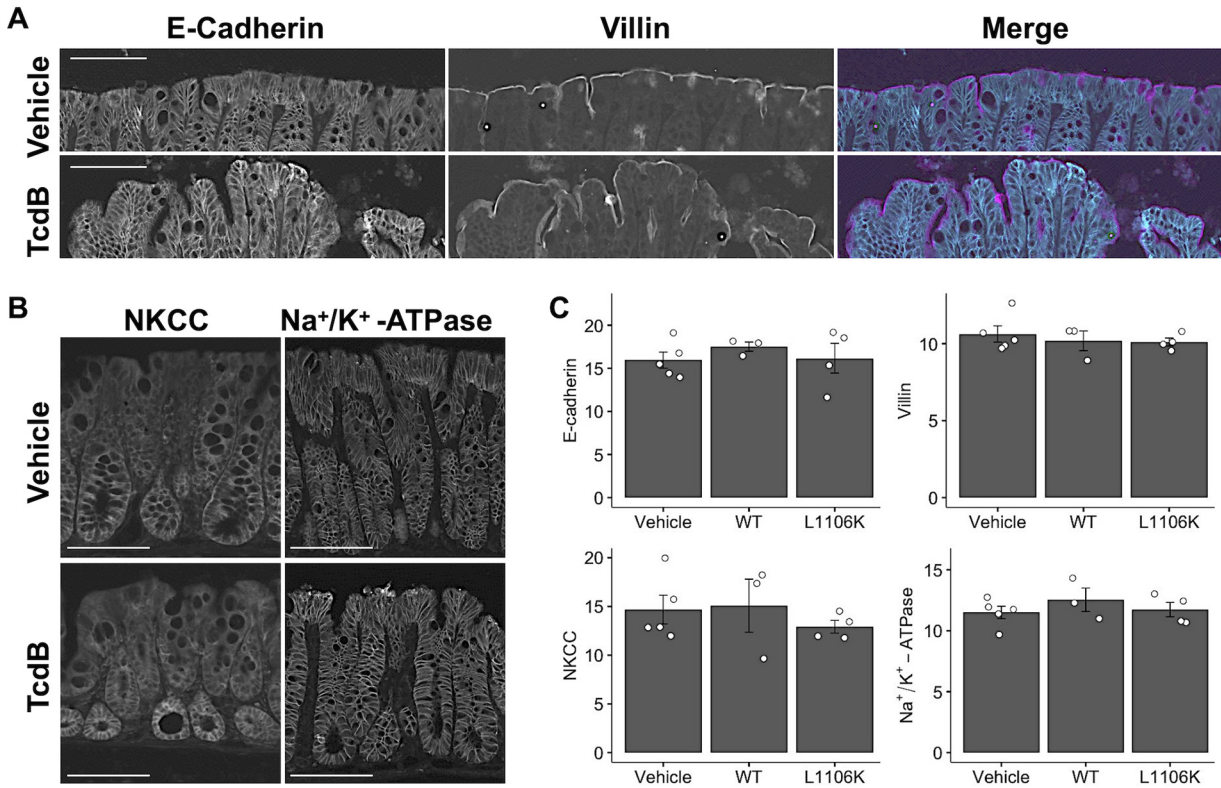


FIG 4 TcdB intoxication affects epithelial architecture but not staining intensity of epithelial cell markers at 4h. (A) Representative immunofluorescence images of mouse colon showing altered epithelial architecture with more luminal irregularities and invaginations than the vehicle control. TcdB mice were instilled with 50 μ g of wild-type TcdB from the VPI 10463 reference strain (WT), and vehicle controls were instilled with PBS only ($n=5$ mice/group). (B) Representative immunofluorescence images showing no changes in crypt base structure as shown by sodium-potassium-chloride channel (NKCC) and sodium-potassium ATPase (Na^+/K^+ -ATPase). Scale bars, 100 μ m. (C) Immunofluorescence quantification of mean pixel intensity in distal colon epithelium. Error bars indicate the SEM ($n=3$ to 5 mice per group); each open circle represents one animal. No comparisons were statistically different by the Kruskal-Wallis test for $P \leq 0.05$.

neutrophils and macrophages in the mouse colon. We also observed how the histopathological scoring for edema, inflammation, and epithelial injury did not clearly differentiate the groups as well as measuring Ly6G^+ cells/crypt (Fig. 5B and C).

DISCUSSION

Here, we present results from an *in vivo* model for *C. difficile* toxin exposure using purified, recombinant TcdA and TcdB. One benefit of using *in vivo* models compared to tissue explants or organoid cultures is the ability to measure neutrophil infiltration during a fully intact acute inflammatory response. Colonic infiltration of neutrophils is a hallmark of CDI, but the effective role of neutrophils is unclear with regard to their beneficial bacterial containment versus their detrimental escalation of cytokine release (34). We observed MPO^+ cell infiltration after intrarectal instillation in mice to be similar to the lower range of MPO^+ cells/crypt in human CDI (Fig. 1B). Adding 5 μ g of TcdA to 5 μ g of TcdB together did not significantly increase the number of MPO^+ cells/crypt or cells/field in the mouse (data not shown), nor did this combination increase the Ly6G^+ cells/crypt compared with 5 μ g of TcdB alone (Fig. 5C). Ly6G is a marker of murine myeloid derived cells and has been used to measure neutrophil recruitment in CDI models (33, 35, 36). It is a sensitive marker for the acute colitis observed with low quantities of TcdA and/or TcdB and is able to differentiate groups better than histopathological scoring (Fig. 5). These observations suggest TcdB induces more acute inflammatory infiltration than TcdA on a per molecule basis.

To directly compare our toxin instillations with *C. difficile* infection, mice were

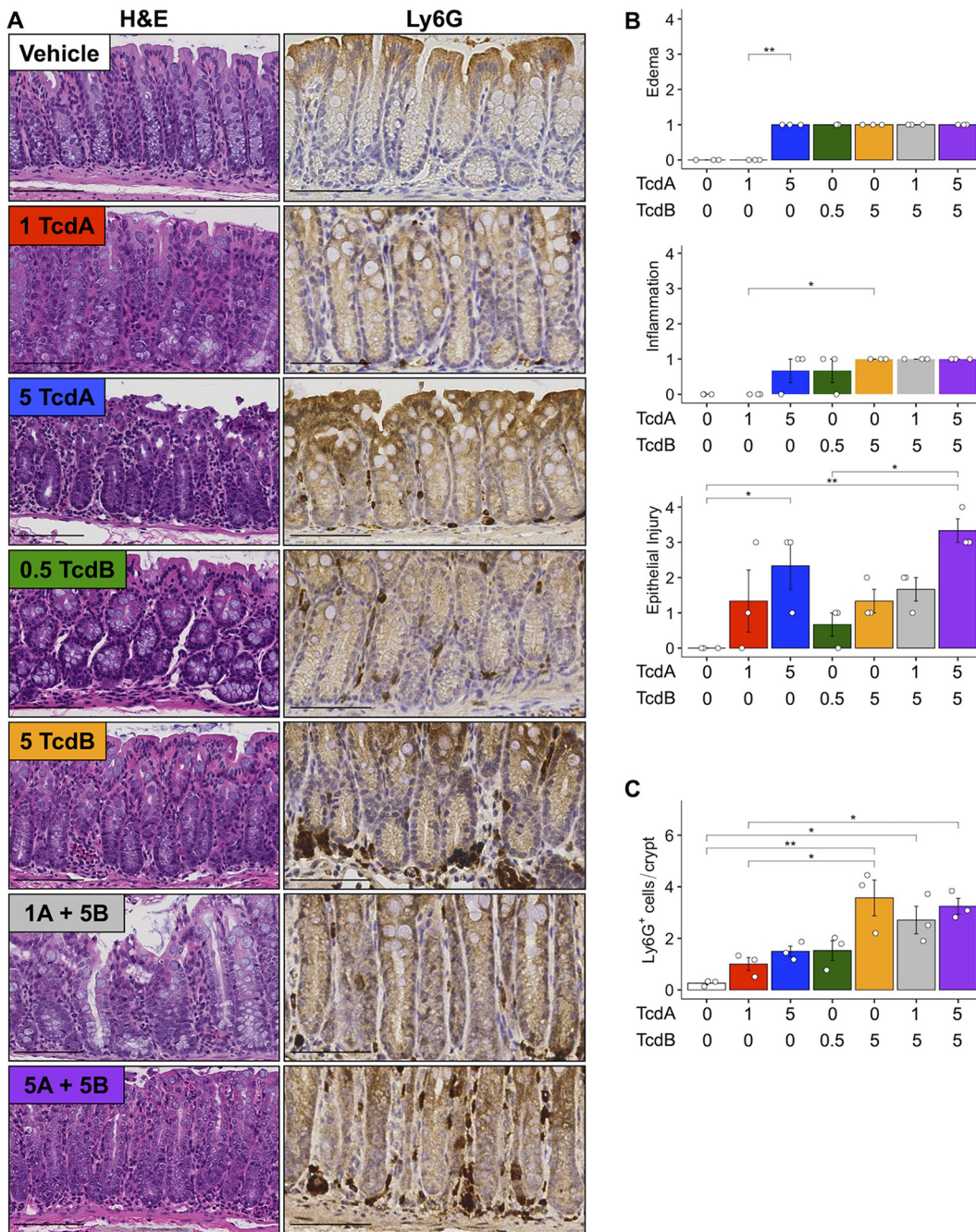


FIG 5 Combination of purified recombinant TcdA and TcdB induces subtle colitis. (A) Representative images of H&E and IHC Ly6G-stained distal mouse colon. Inset labels indicate the μg of TcdA and/or the μg of TcdB intrarectally instilled in the same total volume of $200\ \mu\text{l}$. Scale bar, $100\ \mu\text{m}$. (B) Histopathological scoring as in Fig. 2 and 3. Kruskal-Wallis test was significant with a large effect size for all three subscores: edema, $P = 0.0028$ and $\eta^2 = 1$; inflammation, $P = 0.023$ and $\eta^2 = 0.615$; and epithelial injury, $P = 0.035$ and $\eta^2 = 0.541$. Brackets indicate significance (*, $P \leq 0.05$; **, $P \leq 0.01$ [determined by *post hoc* analysis with Dunn's test]). Error bars indicate the SEM ($n = 3$ mice per group); each open circle represents one animal. Not all significant comparisons are shown with brackets to avoid overplotting. (C) Ly6G⁺ cells/crypt are shown as the means \pm the SEM ($n = 3$ mice per group; each open circle represents one animal). An average of 13.7 crypts were counted per $20\times$ field of view, and 10 fields were counted per mouse. Kruskal-Wallis test was significant with $P = 0.0081$ and $\eta^2 = 0.811$ indicating a large effect size.

pretreated with cefoperazone. The pretreatment did not have a significant impact on histopathological scores compared with water controls (Fig. 3). Compared to R20291 spore gavage, intrarectal instillation of $50\ \mu\text{g}$ of TcdB caused a similar degree of distal inflammation (Fig. 1). The distal colon is most often affected in human disease, but the

largest amount of inflammation in spore-gavaged mice is in the cecum (37, 38). Therefore, another strength of intrarectal instillation is to model distal colitis.

Hirota et al. first published the murine intrarectal instillation model using TcdA and TcdB purified from cultured *C. difficile* (25). In their report, intrarectal instillation of 10 μ g of TcdB alone did not produce significantly more inflammation or epithelial damage than control (25). Here, we showed 5 μ g of purified recombinant TcdB induced significant edema and inflammation (Fig. 2 and 5). Recombinant expression allows for rapid protein purification and may account for the increased potency. Both studies illustrate MPO⁺ cell infiltration and tissue damage in the distal colon. The Hirota study observed animals up to 10 h postinstillation, while we were focused on the initial effect of toxins. We assessed tissue at 4 h postinstillation because we could see histopathological differences without causing morbidity or mortality in the animals. As performed here, intrarectal instillation appears best suited as a model for acute intoxication. Perhaps repeated instillations in the same animal and/or multiday time points could model chronic disease or mucosal restitution.

The ability of TcdB alone to produce a range of histopathological severity from subtle neutrophil infiltration to pseudomembrane formation is valuable for studying CDI pathogenesis and testing therapeutic or preventive interventions. Perhaps the most significant aspect of this recombinant toxin approach is the ability to interrogate easily how changes in toxin structure affect its function. As an example, we have previously shown how a TcdB mutation (¹⁵⁹⁵VNFLQS→¹⁵⁹⁶GFE) abolishing Frizzled binding induces the same histopathological response as wild type (32). Others have used purified recombinant toxin via systemic injection or on explants to show the L543A mutation renders TcdB unable to undergo cysteine protease cleavage while retaining the capacity to induce histological damage (39, 40). In this report, we more thoroughly characterize intrarectal instillation and further illustrate its capabilities using the L1106K and DxD mutant TcdB toxins (Fig. 3 and 4). Neither of these mutant forms were able to induce significantly greater damage than the vehicle control. The L1106K TcdB has been shown concordantly to lack cell rounding or cell killing effects *in vitro* (27, 28). On the other hand, the DxD TcdB has been used *in vitro* and *ex vivo* to demonstrate the glucosyltransferase-independent mechanism for TcdB-induced necrotic cell death (17–19). It is unclear how 50 μ g of DxD TcdB failed to produce significant epithelial injury in the present model, but a recently published report shows isogenic spores lacking glucosyltransferase activity have minimal, if any, colonic inflammation in *C. difficile* infected mouse and hamster models (41). This could be the result of species-specific differences. Published comparisons of human and murine colonic explants exposed to TcdB show mouse tissue having decreased tissue damage (39). Other reasons could include the toxin concentration in colonic tissue being below the threshold for the necrotic effect and/or technical differences in the models. For example, protocols for explant models use reducing agents to degrade mucus prior to TcdB incubation, thus removing a potential protective effect that could permit larger amounts of toxin to contact the epithelial cells than *in vivo*.

C. difficile toxins have been shown to directly affect cell-cell junctions and intestinal permeability (14, 42–44). Other gastrointestinal pathogens, such as *Bacillus fragilis*, *Escherichia coli*, *Klebsiella pneumoniae*, and *Salmonella enterica* serovar Typhimurium, disrupt junctional proteins (45, 46). Using the VPI TcdB and L1106K mutant (both 50 μ g) for intrarectal instillation, we evaluated the epithelial injury by immunofluorescence. The increased luminal invaginations seen by E-cadherin and Villin immunofluorescence illustrate how wild-type TcdB disrupts the epithelial architecture without broadly affecting the intercellular abundance and localization of apical and basolateral proteins NKCC and Na⁺/K⁺-ATP (Fig. 4A and B). This effect is similar to colonic damage induced by diarrheagenic *Escherichia coli* colonization in mice (46). The E-cadherin staining representing adherens junctions and Villin representing the brush border are largely intact (Fig. 4C). Previously, we showed E-cadherin and β -catenin mislocalization in the spore gavage mouse model occurs after 24 h (32). Surprisingly,

pseudomembrane formation can occur at 4 h postinstillation without dramatically affecting adherens junctions in more basally located cells. This observation suggests top-layer cells closest to the lumen are sloughed from the mucosa initially without significant disruption of the underlying cells, which has implications for how host defense mechanisms function during CDI. Future studies will determine these mechanisms by comparing intrarectal instillations to the *C. difficile* spore gavage mouse model of CDI.

MATERIALS AND METHODS

Animals and housing. The Institutional Animal Care and Use Committee at Vanderbilt University Medical Center approved this study. Our laboratory animal facility is AAALAC-accredited and adheres to guidelines set forth in the *Guide for the Care and Use of Laboratory Animals*. The animals' health was assessed daily, and moribund animals were humanely euthanized by CO₂ asphyxiation followed by cervical dislocation. C57BL/6J mice (all females, age 8 to 10 weeks) were purchased from Jackson Laboratories (Bar Harbor, ME) and allowed to assimilate for 1 week to the new facilities, thus avoiding stress-associated responses. Mice were kept in a pathogen-free room with clean bedding and free access to food and water. Cage changes were performed biweekly. Mice had 12-h cycles of light and dark.

Recombinant *C. difficile* toxin purification. TcdA and TcdB were expressed and isolated as previously described (47, 48). Plasmids encoding His-tagged TcdA (pBL282) or TcdB (pBL377) were transformed into *Bacillus megaterium* according to the manufacturer's protocol (MoBiTec). Six liters of Luria-Bertani medium supplemented with 10 mg/liter tetracycline was inoculated with an overnight culture to an optical density at 600 nm (OD₆₀₀) of ~0.1. Cells were grown at 37°C and 220 rpm. Expression was induced with 5 g/liter of D-xylitol once cells reached an OD₆₀₀ of 0.3 to 0.5. After 4 h, the cells were centrifuged and resuspended in 20 mM Tris (pH 8.0), 500 mM NaCl, and protease inhibitors. An EmulsiFlex C3 microfluidizer (Avestin) was used at 15,000 lb/in² twice to generate lysates. Lysates were then centrifuged at 40,000 × g for 20 min. Supernatant containing toxin was passed through a Ni-affinity column (HisTrap FastFlow Crude; GE Healthcare) initially. Further purification was performed using Q-Sepharose anion-exchange chromatography (GE Healthcare) and gel filtration chromatography in 20 mM HEPES (pH 6.9)–50 mM NaCl.

Expression and purification of mutants were performed as for wild-type TcdB. L1106K (pBL682) and DxD (pBL765) mutant TcdB toxins were produced as previously described (19, 27). Q5 High-Fidelity PCR polymerase (M0491) and NEBuilder HiFi DNA Assembly Master Mix (E2621) were used for PCRs and cloning, respectively.

Intrarectal instillation and sample collection. Toxins were prepared in a total volume of 200 μl per instillation. Mice were anesthetized with isoflurane and confirmed to be sedated by toe pinch. The 200-μl instillation was performed over 30 s with a flexible plastic gavage applicator (20 gauge × 30 mm) while lightly pinching closed the anus, which was held for an additional 30 s, as previously described (25). Mice were recovered in their cages. After 4 h, mice were humanely euthanized by CO₂ inhalation. The colon was isolated and dissected away from surrounding visceral tissue. The whole colon was flushed and washed in chilled, sterile 1 × phosphate-buffered saline (PBS) before rolling into a Swiss-roll and fixing in 10% formalin at 4°C for 16 h. Tissue was then washed in 1 × PBS and stored in 70% ethanol prior to paraffin embedding by the VUMC Translational Pathology Shared Resource. IHC staining with antibodies against Ly6G (Novus, NBP1-06691) and MPO (Agilent, A039829-2) was performed as previously described (32). Samples of human *C. difficile*-infected colon tissue were obtained by the Cooperative Human Tissue Network from consented, deidentified donors under the Vanderbilt Institutional Review Board-approved protocol 031078.

Spore preparation and infection. *C. difficile* strain R20291 was obtained from Nigel Minton (Nottingham, UK) and cultured at 37°C in an anaerobic chamber (90% nitrogen, 5% hydrogen, 5% carbon dioxide). Spores were prepared as previously described (26). Briefly, a single colony was picked to inoculate liquid brain heart infusion medium supplemented with 0.5% yeast extract and 0.1% cysteine (BHIS), followed by incubation overnight at 37°C. The next day, 100 μl of that culture was inoculated into 50 ml of Clospore medium, followed by growth for 5 days (49). The culture was centrifuged and washed five times in cold sterile water. Spores were suspended in 1 ml of sterile water and heat treated at 65°C for 20 min to eliminate vegetative cells. Viable spores were enumerated by CFU on BHIS plus taurocholate (0.1%) plates. Spore stocks were stored at 4°C until use. C57BL6/J female mice (8 to 10 weeks old) were treated with cefoperazone (0.5 mg/kg) in sterile drinking water for 5 days, followed by 2 days of untreated water (26). Then, the mice were given a transoral gastric gavage of 100 μl of sterile PBS containing 1 × 10⁹ CFU/ml spores. Mice were monitored daily for morbidity, and daily stool samples were plated on TCCFA (taurocholate, D-cycloserine, cefoxitin, fructose agar) selective media to confirm the *C. difficile* load (26). Mice were humanely euthanized by CO₂ inhalation 4 days postinoculation. The colon was harvested, fixed, and embedded as described above.

Statistical analysis. Statistical testing and graphical representations of the data were performed using the following packages: ggplot2, ggpvr, ggsignif, rstatix, and tidyverse in R version 3.6.3 (50–55). For image quantification, at least 10 fields of view at ×20 magnification were averaged per animal. Statistical significance was set at a $P \leq 0.05$ for all analyses (*, $P \leq 0.05$; **, $P \leq 0.01$; ***, $P \leq 0.001$; ****, $P \leq 0.0001$). The Mann-Whitney-Wilcoxon rank sum (Mann-Whitney) test was used to compare two groups, or the Kruskal-Wallis test was used to calculate significance with *post hoc* analysis using Dunn's test when two groups were compared within multiple comparisons.

ACKNOWLEDGMENTS

Work in the Lacy lab is supported by NIH AI95755 and VA BX002943. Portions of this work were supported by grants R35 CA197570 and GI SPORE P50236733 to Robert J. Coffey, and NIH Training Grant in Gastroenterology T32 DK007673 and a Harrison Society Research Supplement from the VUMC Department of Medicine funded Nicholas O. Markham. Core Services performed through the VUMC Digestive Disease Research Center were supported by NIH grant P30DK058404. These results are solely the responsibility of the authors and do not necessarily represent official views of the NIH.

N.O.M., S.C.B., J.A.S., and D.B.L. conceived the experiments and planned the design. N.O.M., S.C.B., J.A.S., F.C.P.-G., K.O.C., and E.N.L. carried out the experiments. A.K.T. and H. K.K. prepared and purified large amounts of recombinant toxin. N.O.M., S.C.B., J.A.S., M. K.W., R.J.C., and D.B.L. analyzed the data. N.O.M. drafted the manuscript and figures. N. O.M., S.C.B., J.A.S., R.J.C., and D.B.L. edited the manuscript.

We have no financial disclosures or conflicts of interest.

REFERENCES

- Lessa FC, Mu Y, Bamberg WM, Beldavs ZG, Dumyati GK, Dunn JR, Farley MM, Holzbauer SM, Meek JI, Phipps EC, Wilson LE, Winston LG, Cohen JA, Limbago BM, Fridkin SK, Gerding DN, McDonald LC. 2015. Burden of *Clostridium difficile* infection in the United States. *N Engl J Med* 372:825–834. <https://doi.org/10.1056/NEJMoa1408913>.
- Leffler DA, Lamont JT. 2015. *Clostridium difficile* infection. *N Engl J Med* 372:1539–1548. <https://doi.org/10.1056/NEJMra1403772>.
- Ma GK, Brensinger CM, Wu Q, Lewis JD. 2017. Increasing incidence of multiply recurrent *Clostridium difficile* infection in the United States. *Ann Intern Med* 167:152–158. <https://doi.org/10.7326/M16-2733>.
- Centers for Disease Control and Prevention. 2019. Antibiotic resistance threats in the United States. Centers for Disease Control and Prevention, Atlanta, GA.
- Baur D, Gladstone BP, Burkert F, Carrara E, Foschi F, Döbele S, Tacconelli E. 2017. Effect of antibiotic stewardship on the incidence of infection and colonization with antibiotic-resistant bacteria and *Clostridium difficile* infection: a systematic review and meta-analysis. *Lancet Infect Dis* 17:990–1001. [https://doi.org/10.1016/S1473-3099\(17\)30325-0](https://doi.org/10.1016/S1473-3099(17)30325-0).
- Redmond SN, Silva SY, Wilson BM, Cadnum JL, Donskey CJ. 2019. Impact of reduced fluoroquinolone use on *Clostridioides difficile* infections resulting from the fluoroquinolone-resistant ribotype 027 strain in a Veterans Affairs medical center. *Pathog Immun* 4:251–259. <https://doi.org/10.20411/pai.v4i2.327>.
- Mendo-Lopez R, Villafuerte-Gálvez J, White N, Mahoney MV, Kelly CP, Alonso CD. 2020. Recent developments in the management of recurrent *Clostridioides difficile* infection. *Anaerobe* 62:102108. <https://doi.org/10.1016/j.anaerobe.2019.102108>.
- Smits WK, Lyras D, Lacy DB, Wilcox MH, Kuijper EJ. 2016. *Clostridium difficile* infection. *Nat Rev Dis Primers* 2:16020. <https://doi.org/10.1038/nrdp.2016.20>.
- Lyerly DM, Lockwood DE, Richardson SH, Wilkins TD. 1982. Biological activities of toxins A and B of *Clostridium difficile*. *Infect Immun* 35:1147–1150. <https://doi.org/10.1128/IAI.35.3.1147-1150.1982>.
- Lyras D, O'Connor JR, Howarth PM, Sambol SP, Carter GP, Phumoonna T, Poon R, Adams V, Vedantam G, Johnson S, Gerding DN, Rood JI. 2009. Toxin B is essential for virulence of *Clostridium difficile*. *Nature* 458:1176–1179. <https://doi.org/10.1038/nature07822>.
- Kuehne SA, Cartman ST, Heap JT, Kelly ML, Cockayne A, Minton NP. 2010. The role of toxin A and toxin B in *Clostridium difficile* infection. *Nature* 467:711–713. <https://doi.org/10.1038/nature09397>.
- Just I, Selzer J, Wilm M, von Eichel-Streiber C, Mann M, Aktories K. 1995. Glucosylation of Rho proteins by *Clostridium difficile* toxin B. *Nature* 375:500–503. <https://doi.org/10.1038/375500a0>.
- Just I, Wilm M, Selzer J, Rex G, von Eichel-Streiber C, Mann M, Aktories K. 1995. The enterotoxin from *Clostridium difficile* (ToxA) monoglucosylates the Rho proteins. *J Biol Chem* 270:13932–13936. <https://doi.org/10.1074/jbc.270.23.13932>.
- Hecht G, Pothoulakis C, LaMont JT, Madara JL. 1988. *Clostridium difficile* toxin A perturbs cytoskeletal structure and tight junction permeability of cultured human intestinal epithelial monolayers. *J Clin Invest* 82:1516–1524. <https://doi.org/10.1172/JCI113760>.
- Hecht G, Koutsouris A, Pothoulakis C, LaMont JT, Madara JL. 1992. *Clostridium difficile* toxin B disrupts the barrier function of T84 monolayers. *Gastroenterology* 102:416–423. [https://doi.org/10.1016/0016-5085\(92\)90085-d](https://doi.org/10.1016/0016-5085(92)90085-d).
- Pruitt RN, Lacy DB. 2012. Toward a structural understanding of *Clostridium difficile* toxins A and B. *Front Cell Infect Microbiol* 2:28.
- Chumbler NM, Farrow MA, Lapierre LA, Franklin JL, Haslam DB, Haslam D, Goldenring JR, Lacy DB. 2012. *Clostridium difficile* toxin B causes epithelial cell necrosis through an autoproduct-independent mechanism. *PLoS Pathog* 8:e1003072. <https://doi.org/10.1371/journal.ppat.1003072>.
- Farrow MA, Chumbler NM, Lapierre LA, Franklin JL, Rutherford SA, Goldenring JR, Lacy DB. 2013. *Clostridium difficile* toxin B-induced necrosis is mediated by the host epithelial cell NADPH oxidase complex. *Proc Natl Acad Sci U S A* 110:18674–18679. <https://doi.org/10.1073/pnas.1313658110>.
- Chumbler NM, Farrow MA, Lapierre LA, Franklin JL, Lacy DB. 2016. *Clostridium difficile* toxins TcdA and TcdB cause colonic tissue damage by distinct mechanisms. *Infect Immun* 84:2871–2877. <https://doi.org/10.1128/IAI.00583-16>.
- Carter GP, Chakravorty A, Nguyen TAP, Mileto S, Schreiber F, Li L, Howarth P, Clare S, Cunningham B, Sambol SP, Cheknis A, Figueroa I, Johnson S, Gerding D, Rood JI, Dougan G, Lawley TD, Lyras D. 2015. Defining the roles of TcdA and TcdB in localized gastrointestinal disease, systemic organ damage, and the host response during *Clostridium difficile* infections. *mBio* 6:e00551-15. <https://doi.org/10.1128/mBio.00551-15>.
- Shin B-M, Kuak EY, Yoo SJ, Shin WC, Yoo HM. 2008. Emerging toxin A⁻B⁺ variant strain of *Clostridium difficile* responsible for pseudomembranous colitis at a tertiary care hospital in Korea. *Diagn Microbiol Infect Dis* 60:333–337. <https://doi.org/10.1016/j.diagmicrobio.2007.10.022>.
- Kim J, Kim Y, Pai H. 2016. Clinical characteristics and treatment outcomes of *Clostridium difficile* infections by PCR ribotype 017 and 018 strains. *PLoS One* 11:e0168849. <https://doi.org/10.1371/journal.pone.0168849>.
- Hung Y-P, Huang I-H, Lin H-J, Tsai B-Y, Liu H-C, Liu H-C, Lee J-C, Wu Y-H, Tsai P-J, Ko W-C. 2016. Predominance of *Clostridium difficile* ribotypes 017 and 078 among toxigenic clinical isolates in southern Taiwan. *PLoS One* 11:e0166159. <https://doi.org/10.1371/journal.pone.0166159>.
- Cairns MD, Preston MD, Lawley TD, Clark TG, Stabler RA, Wren BW. 2015. Genomic epidemiology of a protracted hospital outbreak caused by a toxin A-negative *Clostridium difficile* sublineage PCR ribotype 017 strain in London, England. *J Clin Microbiol* 53:3141–3147. <https://doi.org/10.1128/JCM.00648-15>.
- Hirota SA, Iablokov V, Tulk SE, Schenck LP, Becker H, Nguyen J, Bashir SA, Dingle TC, Laing A, Liu J, Li Y, Bolstad J, Mulvey GL, Armstrong GD, MacNaughton WK, Muruve DA, MacDonald JA, Beck PL. 2012. Intrarectal instillation of *Clostridium difficile* toxin A triggers colonic inflammation and tissue damage: development of a novel and efficient mouse model of *Clostridium difficile* toxin exposure. *Infect Immun* 80:4474–4484. <https://doi.org/10.1128/IAI.00933-12>.
- Theriot CM, Koumpouras CC, Carlson PE, Bergin II, Aronoff DM, Young VB. 2011. CFOPerazone-treated mice as an experimental platform to assess differential virulence of *Clostridium difficile* strains. *Gut Microbes* 2:326–334. <https://doi.org/10.4161/gmic.19142>.
- Zhang Z, Park M, Tam J, Auger A, Beilhartz GL, Lacy DB, Melnyk RA. 2014.

- Translocation domain mutations affecting cellular toxicity identify the *Clostridium difficile* toxin B pore. *Proc Natl Acad Sci U S A* 111:3721–3726. <https://doi.org/10.1073/pnas.1400680111>.
28. Hamza T, Zhang Z, Melnyk RA, Feng H. 2016. Defective mutations within the translocation domain of *Clostridium difficile* toxin B impair disease pathogenesis. *Pathog Dis* 74:ftv098. <https://doi.org/10.1093/femspd/ftv098>.
 29. Busch C, Hofmann F, Selzer J, Munro S, Jeckel D, Aktories K. 1998. A common motif of eukaryotic glycosyltransferases is essential for the enzyme activity of large clostridial cytotoxins. *J Biol Chem* 273:19566–19572. <https://doi.org/10.1074/jbc.273.31.19566>.
 30. Reinert DJ, Jank T, Aktories K, Schulz GE. 2005. Structural basis for the function of *Clostridium difficile* toxin B. *J Mol Biol* 351:973–981. <https://doi.org/10.1016/j.jmb.2005.06.071>.
 31. Jank T, Giesemann T, Aktories K. 2007. *Clostridium difficile* glycosyltransferase toxin B-essential amino acids for substrate binding. *J Biol Chem* 282:35222–35231. <https://doi.org/10.1074/jbc.M703138200>.
 32. Mileto SJ, Jardé T, Childress KO, Jensen JL, Rogers AP, Kerr G, Hutton ML, Sheedlo MJ, Bloch SC, Shupe JA, Horvay K, Flores T, Engel R, Wilkins S, McMurrick PJ, Lacy DB, Abud HE, Lyras D. 2020. *Clostridioides difficile* infection damages colonic stem cells via TcdB, impairing epithelial repair and recovery from disease. *Proc Natl Acad Sci U S A* 117:8064–8073. <https://doi.org/10.1073/pnas.1915255117>.
 33. McDermott AJ, Falkowski NR, McDonald RA, Frank CR, Pandit CR, Young VB, Huffnagle GB. 2017. Role of interferon- γ and inflammatory monocytes in driving colonic inflammation during acute *Clostridium difficile* infection in mice. *Immunology* 150:468–477. <https://doi.org/10.1111/imm.12700>.
 34. Jose S, Madan R. 2016. Neutrophil-mediated inflammation in the pathogenesis of *Clostridium difficile* infections. *Anaerobe* 41:85–90. <https://doi.org/10.1016/j.anaerobe.2016.04.001>.
 35. McDermott AJ, Falkowski NR, McDonald RA, Pandit CR, Young VB, Huffnagle GB. 2016. Interleukin-23 (IL-23), independent of IL-17 and IL-22, drives neutrophil recruitment and innate inflammation during *Clostridium difficile* colitis in mice. *Immunology* 147:114–124. <https://doi.org/10.1111/imm.12545>.
 36. El-Zaatari M, Chang Y-M, Zhang M, Franz M, Shreiner A, McDermott AJ, van der Sluijs KF, Lutter R, Grasberger H, Kamada N, Young VB, Huffnagle GB, Kao JY. 2014. Tryptophan catabolism restricts IFN- γ -expressing neutrophils and *Clostridium difficile* immunopathology. *J Immunol* 193:807–816. <https://doi.org/10.4049/jimmunol.1302913>.
 37. Chen X, Katchar K, Goldsmith JD, Nanthakumar N, Cheknis A, Gerding DN, Kelly CP. 2008. A mouse model of *Clostridium difficile*-associated disease. *Gastroenterology* 135:1984–1992. <https://doi.org/10.1053/j.gastro.2008.09.002>.
 38. Tedesco FJ, Corless JK, Brownstein RE. 1982. Rectal sparing in antibiotic-associated pseudomembranous colitis: a prospective study. *Gastro* 83:1259–1260. [https://doi.org/10.1016/S0016-5085\(82\)80136-4](https://doi.org/10.1016/S0016-5085(82)80136-4).
 39. Wang J, Ortiz C, Fontenot L, Mukhopadhyay R, Xie Y, Chen X, Feng H, Pothoulakis C, Koon HW. 2020. Therapeutic mechanism of macrophage inflammatory protein 1 α neutralizing antibody (CCL3) in *Clostridium difficile* infection in mice. *J Infect Dis* 221:1623–1635. <https://doi.org/10.1093/infdis/jiz640>.
 40. Li S, Shi L, Yang Z, Zhang Y, Perez-Cordon G, Huang T, Ramsey J, Oezguen N, Savidge TC, Feng H. 2015. Critical roles of *Clostridium difficile* toxin B enzymatic activities in pathogenesis. *Infect Immun* 83:502–513. <https://doi.org/10.1128/IAI.02316-14>.
 41. Bilverstone TW, Garland M, Cave RJ, Kelly ML, Tholen M, Bouley DM, Kaye P, Minton NP, Bogoyo M, Kuehne SA, Melnyk RA. 2020. The glucosyltransferase activity of *C. difficile* toxin B is required for disease pathogenesis. *PLoS Pathog* 16:e1008852. <https://doi.org/10.1371/journal.ppat.1008852>.
 42. Pothoulakis C. 2000. Effects of *Clostridium difficile* toxins on epithelial cell barrier. *Ann N Y Acad Sci* 915:347–356. <https://doi.org/10.1111/j.1749-6632.2000.tb05263.x>.
 43. Lawrence JP, Brevetti L, Obiso RJ, Wilkins TD, Kimura K, Soper R. 1997. Effects of epidermal growth factor and *Clostridium difficile* toxin B in a model of mucosal injury. *J Pediatr Surg* 32:430–433. [https://doi.org/10.1016/S0022-3468\(97\)90598-4](https://doi.org/10.1016/S0022-3468(97)90598-4).
 44. Leslie JL, Huang S, Opp JS, Nagy MS, Kobayashi M, Young VB, Spence JR. 2015. Persistence and toxin production by *Clostridium difficile* within human intestinal organoids result in disruption of epithelial paracellular barrier function. *Infect Immun* 83:138–145. <https://doi.org/10.1128/IAI.02561-14>.
 45. Lacombe S, Hutton ML, Riley TV, Abud HE, Lyras D. 2018. Diverse bacterial species contribute to antibiotic-associated diarrhoea and gastrointestinal damage. *J Infect* 77:417–426. <https://doi.org/10.1016/j.jinf.2018.06.006>.
 47. Yang G, Zhou B, Wang J, He X, Sun X, Nie W, Tzipori S, Feng H. 2008. Expression of recombinant *Clostridium difficile* toxin A and B in *Bacillus megaterium*. *BMC Microbiol* 8:192. <https://doi.org/10.1186/1471-2180-8-192>.
 48. Pruitt RN, Chambers MG, Ng KK-S, Ohi MD, Lacy DB. 2010. Structural organization of the functional domains of *Clostridium difficile* toxins A and B. *Proc Natl Acad Sci U S A* 107:13467–13472. <https://doi.org/10.1073/pnas.1002199107>.
 49. Perez J, Springthorpe VS, Sattar SA. 2011. Clospore: a liquid medium for producing high titers of semi-purified spores of *Clostridium difficile*. *J AOAC Int* 94:618–626. <https://doi.org/10.1093/jaoac/94.2.618>.
 50. Wickham H. 2016. ggplot2: elegant graphics for data analysis. Springer-Verlag, New York, NY.
 51. Kassambara A. 2020. ggpubr: “ggplot2”-based publication ready plots. <https://cran.r-project.org/web/packages/ggpubr/index.html>.
 52. Ahlmann-Eltze C. 2019. ggsignif: significance brackets for “ggplot2.” <https://CRAN.R-project.org/package=ggsignif>.
 53. Kassambara A. 2020. rstatix: Pipe-Friendly framework for basic statistical tests. <https://cran.r-project.org/web/packages/rstatix/index.html>.
 54. Wickham H, Averick M, Bryan J, Chang W, McGowan L, François R, Grolemund G, Hayes A, Henry L, Hester J, Kuhn M, Pedersen T, Miller E, Bache S, Müller K, Ooms J, Robinson D, Seidel D, Spinu V, Takahashi K, Vaughan D, Wilke C, Woo K, Yutani H. 2019. Welcome to the Tidyverse. *JOSS* 4:1686. <https://doi.org/10.21105/joss.01686>.
 55. R Core Team. 2020. R: a language and environment for statistical computing. R Foundation for Statistical Computing, Vienna, Austria.